Characterization of PV panel and global optimization of its model parameters using genetic algorithm

M.S. Ismail [a,*], M. Moghavvemi [a,b], T.M.I. Mahlia [c,d]

[a] Department of Electrical Engineering, University of Malaya, 50603 Kuala Lumpur, Malaysia
[b] Faculty of Electrical and Computer Engineering, University of Tehran, Tehran, Iran
[c] Department of Mechanical Engineering, Universiti Tenaga Nasional, 43000 Kajang, Selangor, Malaysia
[d] Department of Mechanical Engineering, Syiah Kuala University, Banda Aceh 23111, Indonesia

ABSTRACT

This paper details an improved modeling technique for a photovoltaic (PV) module; utilizing the optimization ability of a genetic algorithm, with different parameters of the PV module being computed via this approach. The accurate modeling of any PV module is incumbent upon the values of these parameters, as it is imperative in the context of any further studies concerning different PV applications. Simulation, optimization and the design of the hybrid systems that include PV are examples of these applications. The global optimization of the parameters and the applicability for the entire range of the solar radiation and a wide range of temperatures are achievable via this approach. The Manufacturer's Data Sheet information is used as a basis for the purpose of parameter optimization, with an average absolute error fitness function formulated; and a numerical iterative method used to solve the voltage-current relation of the PV module. The results of single-diode and two-diode models are evaluated in order to ascertain which of them are more accurate. Other cases are also analyzed in this paper for the purpose of comparison. The Matlab–Simulink environment is used to simulate the operation of the PV module, depending on the extracted parameters. The results of the simulation are compared with the Data Sheet information, which is obtained via experimentation in order to validate the reliability of the approach. Three types of PV modules, using different technologies, are tested for the purpose of this validation, and the results confirm the accuracy and reliability of the approach developed in this study. The effectiveness of the model developed by this approach to predict the performance of the PV system under partial shading conditions was also validated.

© 2013 Elsevier Ltd. All rights reserved.

1. Introduction

Photovoltaic systems are one of the most popular renewable energy sources in today's world. There are ubiquitous in numerous settings, be it urban or rural [1–3]. Due to the many factors and benefits, both the public and private sectors are showing a tremendous amount of interest in the potential and capability of energy generation from these devices [4–7]. One of the major advantages of PV technology is its long lifecycle time, with low operation and maintenance costs, due to the fact that it does not rely on a minimal number of moving parts. Furthermore, this technology heralds a clean and environmentally-friendly energy source. Another salient feature of the PV technology is its modularity, where instead of installing a whole new system whenever required; a current system can be upgraded accordingly within a short period of time [8–17]. Its benefits

and flexibility makes it ideal for space and earth applications [16,18], and it is expected to grow in the near future, from small PV stand-alone site applications, to large PV grid connected systems [19–21].

As previously mentioned, a PV power system is one of the more important renewable energy sources. Due to its importance, large PV power systems have been installed in multiple countries. However, due to the high initial capital needed for this technology, the optimal utilization of the solar energy should be insured, and precise studies and simulation of the PV power system shall be performed prior to its installation [22–24]. The modeling of the PV module represents the important task in the whole PV system pre-installation procedure.

Modeling of the PV cell is a mathematical description of the PV output current–voltage (I–V), and power–voltage (P–V) relations. A general equivalent circuit (model) that represents the operation of the PV cell is illustrated in Fig. 1. This model is called a single-diode model. A more detailed model is a two-diode model, which uses two diodes to express the P–N junction effect, and this model is shown in Fig. 2.

* Corresponding author. Mobile: 60 12 239 4312; fax: +60 37 956 1378.
E-mail addresses: mahmoud_kafa@yahoo.com, mahmoud@um.edu.my (M.S. Ismail).

Nomenclatures

a	idealityfactor
a_1	ideality factor of diode 1
a_2	ideality factor of diode 2
DV	decision vector
DV_{1d}	decision vector-single-diode model
DV_{2d}	decision vector-two-diode model
$DV_{1d\text{-}m}$	decision vector-modified single-diode model
$DV_{2d\text{-}m}$	decision vector-modified two-diode model
$Error_{ave}$	average absolute error
G	solar radiation (W/m^2)
G_j	solar radiation (W/m^2) at point j
G_{STC}	solar radiation (W/m^2) at standard test conditions
I_{D1}	current of diode 1 (A)
I_{D2}	current of diode 2 (A)
I_j (curve)	current (A) read from curve at point j
I_{mp}	current (A) at maximum power point
$I_{mp\text{-}STC}$	current (A) at maximum power point at standard test conditions
I_0	saturation current (A)
I_{01}	saturation current (A) of diode 1
I_{02}	saturation current (A) of diode 2
I_{ph}	photon current (A)
$I_{Ph\text{-}STC}$	photon current at standard test conditions
I_{PV}	output PV current (A)
I_{pvn}	present value of output PV current (A)
$Ipvn + 1$	next value of output PV current (A)
I_{SC-STC}	short circuit current at standard test conditions (A)
I–V	current–voltage
K	Boltzmann constant (=1.38065 × 10^{-23} J/K)
K_I	current temperature coefficient (A/°C)
K_V	voltage temperature coefficient (V/°C)
Ns	number of series cells in one PV panel
p	number of points
PV	photovoltaic
P-V	power–voltage
Q	electron charge (=1.6021765 × 10^{-19} C)
R_p	shunt resistance (Ω)
R_S	series resistance (Ω)
T	P–N junction temperature (K)
T_j	ambient temperature at point j (K)
T_{STC}	temperature at standard test conditions (=25 °C or 298.15 K)
V_j	voltage at point j (V)
V_{mp}	voltage at maximum power point (V)
$V_{mp\text{-}STC}$	voltage at maximum power point (V) at standard test conditions
$V_{OC\text{-}STC}$	voltage at open circuit (V) at standard test conditions
V_{PV}	output PV voltage (V)
V_T	thermal voltage (V)
V_{T1}	thermal voltage of diode 1
V_{T2}	thermal voltage of diode 2

The PV technology is readily available in the current market. Due to the sheer number of the different types of PV technology available, the precise evaluation of different parameters of the equivalent circuit in real conditions of operation is imperative for an accurate and reliable modeling and simulation of PV systems [19,22,25].

Chouder et al. [19] and Sera et al. [26] used a single-diode model to simulate the operation of a PV module. The authors depended on the manufacturer's data to initially determine the values of both the series and shunt resistances. Moreover, the ideality factor, saturation current and photon current are also needed for this evaluation, in accordance to the relations they used. Most of the manufacturers do not provide values for these parameters, so an assumption for each of these parameters or iterative method shall
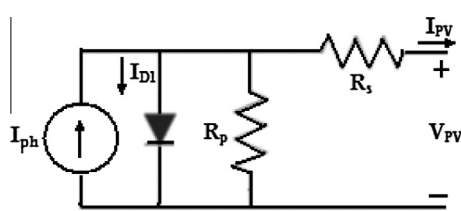

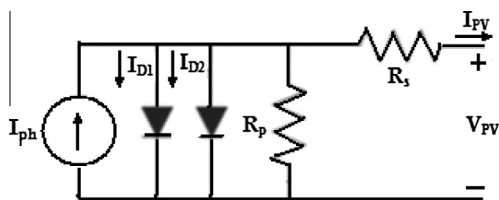**Fig. 1.** Single-diode PV equivalent circuit.

Fig. 2. Two-diode PV equivalent circuit.

be made. In the proposed genetic algorithm approach, part of these variables and quantities are included in the decision vector of the genetic algorithm, while others are computed according to different equations, which will be discussed at a later stage of this paper.

Ishaque et al. [22] used a two-diode model for the purpose of modeling a PV cell. This model computes more parameters, which necessitates certain assumption in the effort to simplify computations. The iterative method was also used to calculate both the series and shunt resistances.

Ishaque and Salam [27] used a differential evolution method to determine the model parameters of the PV modules. The effects of temperature and irradiance were included, and the values for the different parameters were calculated for each temperature or irradiance. The global optimization of these parameters fitting any irradiance or temperature is not calculated in the presented approach in this reference. Furthermore, ways to calculate the model's parameters when simultaneous change of temperature and irradiance occurs were also not discussed in this reference.

Shahat [28] developed a model for PV in order for it to be used for maximum power point identification. In this approach, the author depended on the assumed values for the ideality factor, and also on the assumption that the datasheet curve of the PV panel is provided by the manufacturer to graphically calculate the series resistance. The genetic algorithm used in the approach in this reference is utilized only to determine the maximum power point.

Zagrouba et al. [29] presented a method to identify the electrical parameters of PV solar cells and modules. A single-diode model was used in this study. Results produced by the Pasan cell tester software were used to validate the values obtained for the PV cell's parameters. This software does not provide values for all parameters. Furthermore, the temperature and radiation variations were not taken into account while using this approach, and as mentioned earlier; the values of these parameters are influenced by variations in temperature and radiation.

Weidong et al. [30] used a simplified single-diode model to determine the parameters of a PV module. The shunt resistance was neglected in their approach. The graphical relationships between both series resistance and ideality factor with temperature changes were also presented. These relations were used for the evaluation of the parameters. For validation purposes, the authors took into account the maximum power point at certain radiation only as the temperature changes; and as proven by authors of Ref. [27] , the values of these parameters vary with the variation of the radiation. As previously mentioned, not only the maximum power point is taken into account in our approach; other points on the I–V curve at different temperatures and radiation levels are taken into account as well.

Villalva et al. [31] suggested and developed an approach to find the parameters of a single-diode model of a PV module. An effective method was proposed to fit the mathematical I–V curve to the three characterizing points of any PV module (Isc point, Voc point and maximum power point). The model was validated by comparison of simulation results with two practical PV arrays. In order to calculate the saturation current, a value for the ideality factor was assumed, and remains unmodified later in the model. Furthermore, an iterative method was used to calculate both the series and shunt resistances. The iteration is performed until certain values of the series or shunt resistances render the power generated by PV matches the maximum power at certain temperatures and radiation. As it is known, the values of these resistances depend on both temperature and radiation [27], so the values obtained may not fit the model, especially at low values of radiation (less than 400 W/m^2). In the developed approach in this paper, the ideality factor, series and shunt resistances are part of the decision vector that are to be computed using genetic algorithm. Furthermore, different points at different radiation levels and temperatures were used in calculations, and is not only limited to the maximum power point at certain radiation or temperatures.

Jervase et al. [32] proposed a technique for improving the accuracy of the solar cell's parameters. The developed approach hinged on the fact that the specified values of these parameters were given or calculated using one of the known extraction methods at certain conditions. The proposed genetic algorithm was then used to refine these values. This may be applicable from a physical point of view, but it is inapplicable for PV applications, where other data are usually provided by the manufacturer. Furthermore, the variations of temperature and radiation were not taken into account in this context.

Almonacid et al. [33] developed an artificial neural network approach to generate V-I curves of silicon-crystalline PV modules for any radiation or temperature values. This approach is capable of predicting the performance of the PV module, but a mathematical model involving the different parameters is not provided by this approach.

The ability of the PV model to predict the performance of the PV system under partial shading should also be fulfilled. Several researches have studied the performance of the PV panel under partial shading [22,34,35]. The effectiveness of the two diode model developed in Ref. [22] was also validated under partial shading conditions. The performance was checked under different shading patterns. Shaiek et al. [34] used a single-diode to express the operation of the PV module, and the genetic algorithm was utilized to search for the global maximum power point under the shading effect. In this work, the simulations were conducted with two panels connected in series, where one of them was assumed to be partially shaded. The simulations showed the ability of the genetic algorithm to realize the global maximum power point. A way to obtain values of the PV model was not mentioned in this study, which prompted the authors to use typical values for these parameters.

The previous works discussed above indicated that the ideality factor is one of the parameters that require major analysis for estimation. According to Ref. [28], a more accurate value for this parameter can be obtained by curve fitting, or by trial and error. This value estimation is inaccurate, due to the fact that it may fit a certain I–V curve only at certain temperatures or radiation, but is not inclusive of all temperatures and radiation levels.

In this study, the global optimization ability of the genetic algorithm was utilized in order to obtain the parameters of the PV model. Obtaining values for these parameters that are applicable for the entire range of the solar radiation and a wide range of temperatures forms the purpose of this study. In order to achieve this, different points on the I–V curve at different temperatures and different radiation levels were used to calculate the optimized error function, and Matlab–Simulink was used to build the simulation model, depending on the values of the parameters obtained by the optimization algorithm. The results of the simulation were compared with real data obtained from the manufacturer's datasheet(s) for validation purposes. Different cases were also studied in this paper for comparison purposes.

In a nutshell, the approach developed in this study realized the global optimization of the parameters of the PV model, with the variation of temperature and radiation, which affects these values that are being taken into consideration.

2. Materials and methods

2.1. Genetic algorithms

The genetic algorithms are methods used to solve constrained and unconstrained optimization problems. They have been used to solve optimization problems in engineering and the sciences [32,36], and are considered global methods for the purpose of optimization.

The population of individual solutions is repeatedly modified by genetic algorithm. Individuals are randomly selected at each step from the current population, and these individuals are used as parents to generate the children of the next generation [28,37].

Three main rules are used by genetic algorithm at each step to form the next generation from the present population, and these rules are: selection rules to select the individuals (parents) that is considered the source for the next generation, crossover rules that combine two parents to produce children for the next generation, and mutation rules that randomly apply changes to individual parents to produce children [28].

In this paper, the genetic algorithm was programmed in two ways: MATLAB optimization Toolbox, and developed MATLAB code. This was done for the purpose of comparison.

2.1.1. Genetic algorithm using MATLAB global optimization Toolbox

This method involves a MATLAB code that is developed in order to form the optimization fitness function; the optimization Toolbox utilizes this file to run the genetic algorithm solver. Different terminologies shall be specified for the purpose of optimization. Before specifying certain values for each of these terminologies, all of them were tested with regards to the accuracy of the results and their corresponding computation time. The following MATLAB prescribed terminologies are selected in the genetic algorithm Toolbox for the purpose of optimization in this paper:

- Population type: double vector with populations size = 20.
- Fitness scaling: rank.
- Selection function: stochastic uniform reproduction.
- Reproduction: elite count: default (2), crossover fraction: default (0.8).

- Mutation function: adaptive feasible.
- Crossover function: scattered migration.
- Migration: direction: forward, fraction: default (0.2), interval: default (20).
- Algorithm settings: as default.
- Stopping criteria (defaults): generations: 100.

2.1.2. Genetic algorithm using developed MATLAB code

As an alternative to the optimization Toolbox, a MATLAB code is duly developed. This code includes both the genetic algorithm programming and the programming of the optimization fitness function. In this code, the initial population generation is formed by randomly generating population members (possible solutions). Each possible solution is a code of the decision vector, taking into account the upper and lower constraints. This initial generation evolves through successive iterations, and members of each generation are evaluated in order to calculate the fitness average error

function, with the member possessing the least error being selected. Fig. 3 details the flowchart of the genetic algorithm process.

In this method, and after performing many executions, it was discovered that a population size of 30 is adequate for the purpose of this paper, while the number of generations required to give the most optimal solution is 100. In most cases, the number of required generations is less than 60. It is also found that 0.9 is an appropriate rate for both cross-over and mutation.

2.2. Simulation

After using the genetic algorithm to obtain the optimized values for the different PV model parameters that is needed to construct the decision vector, Matlab–Simulink is the simulation environment that is used to simulate the operation of this PV module. The basic numerical model for the PV module used in the simulation is shown in Fig. 4. If a single-diode model is used, then the
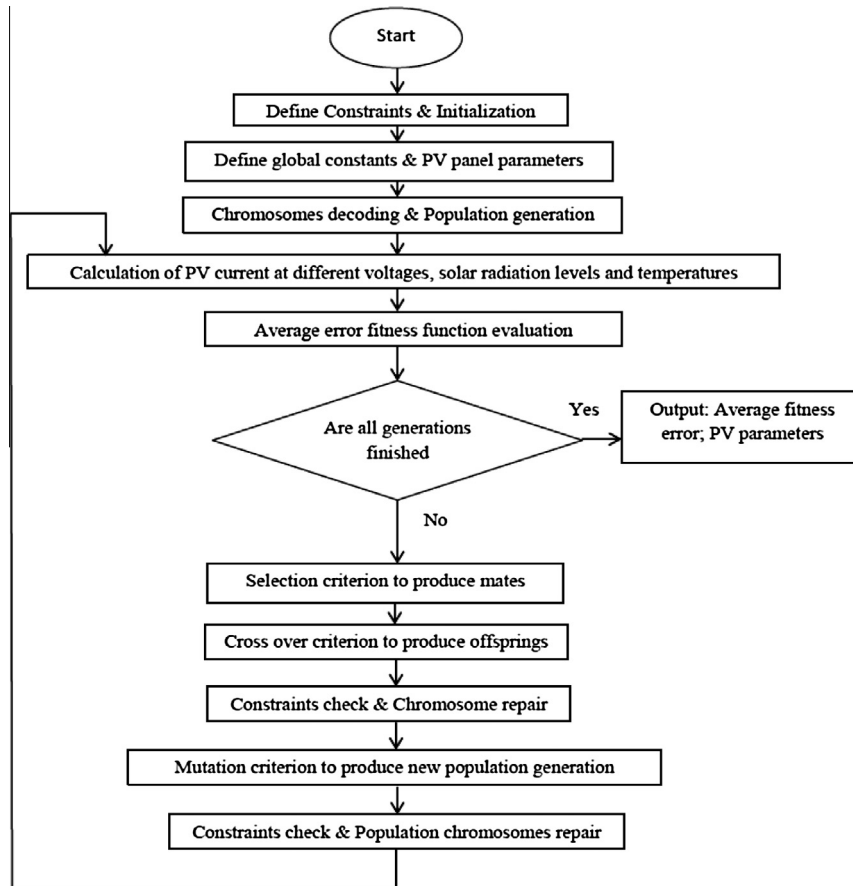

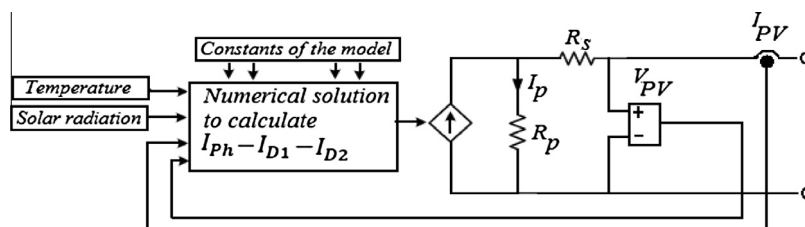**Fig. 3.** Flow chart of the genetic algorithm.

Fig. 4. Numerical model of the PV module.

contents of the numerical solution box in the figure become $I_{ph} - I_{DI}$.

Fig. 5 shows the details of a Matlab–Simulink model of a PV-equivalent circuit. This block forms part of a whole PV system, and is illustrated in Fig. 6. In this study, the purpose of this system is to calculate the I–V and P–V characteristics of a typical PV panel for validation purposes. This simulation model can be considered part of a total system, and in addition to the PV panel, this system may include a charge regulator, inverter, or any conditioning circuit.

Fig. 5 represents the inside details of the block called PV panel in Fig. 6. The other details of Fig. 6 are for measuring and displaying signals, where the two external outputs of this block are called (V + PV and V − PV), and are actually used for both voltage and current sensing in the simulation block, while the two additional outputs appearing in Fig. 5 are internal outputs used for the calculation of the PV panel current ($Ipv = I_{ph} - I_{D1}$).

Different constants, variables and parameters of the model are defined through the MATLAB code executed in parallel with the Simulink model.

3. Theory and calculations

3.1. Mathematical modeling

Any model that is adopted to characterize the PV panel involves several parameters that need to be calculated, depending on the experimental data. The number of these parameters differs in accordance to the adopted model. A single-diode model provides a good compromise between accuracy and simplicity [31], and it has been used by several authors in previous research works [31,34]. Its effectiveness is proven, especially in the simulation of PV modules with power converters. A two-diode model that takes into account different conditions of the operation of a PV panel is also used by different researchers for the purpose of modeling PV panels.

The approach to calculate different parameters characterizing the I–V curve is as follows:

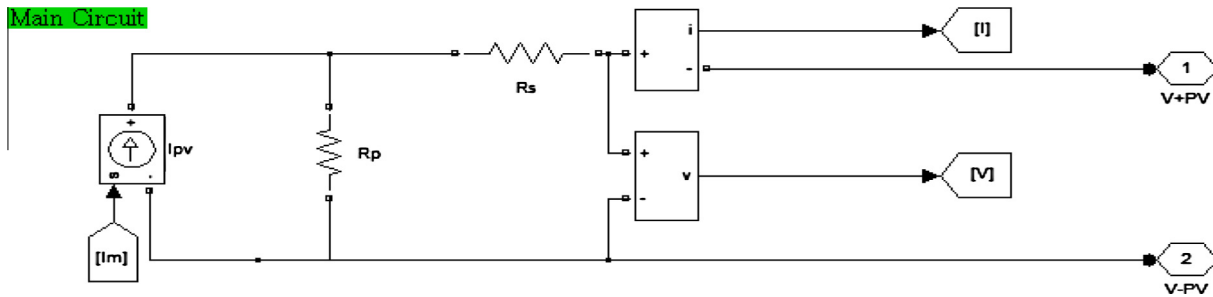$$I_{PV} = I_{Ph} - I_{D1} - I_{D2} - \left(\frac{V_{PV} + I_{PV}R_s}{R_P} \right) \tag{1}$$
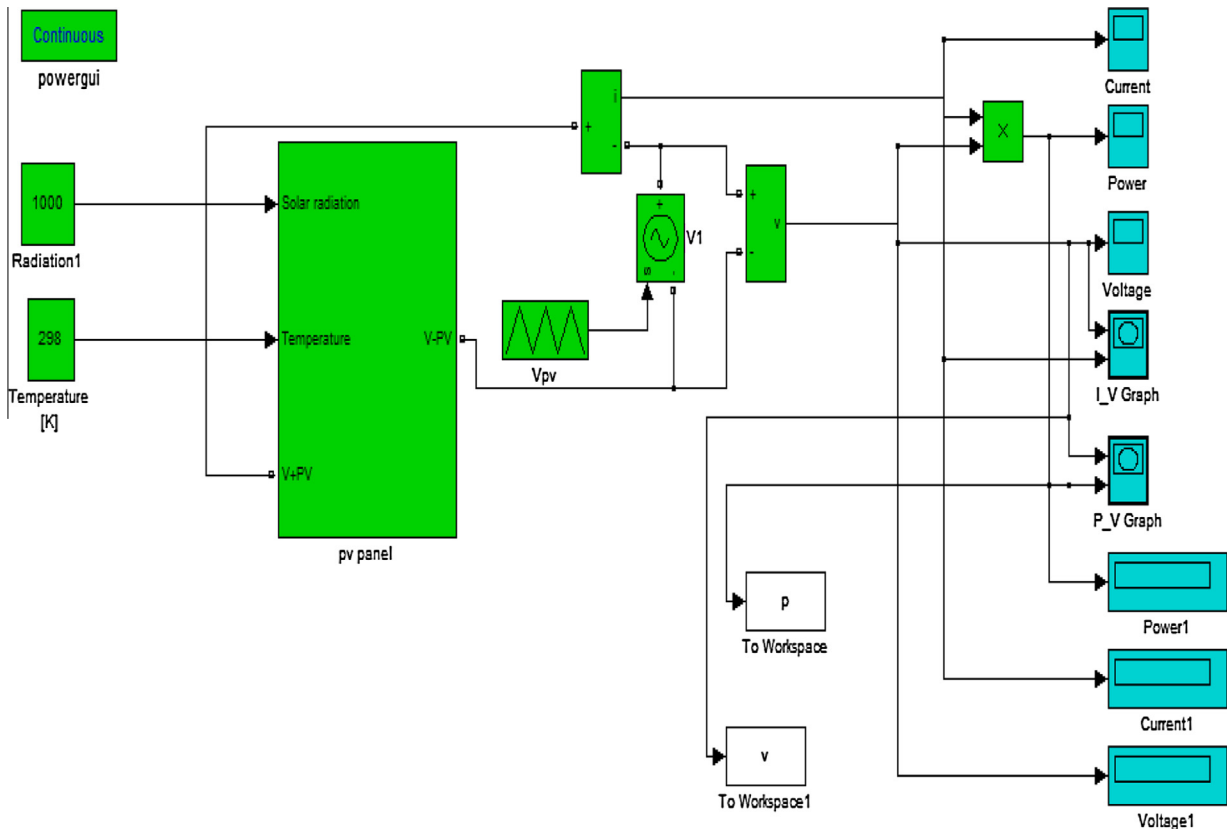
Fig. 5. Main block of Matlab–Simulink model.

Fig. 6. The PV system simulated by Matlab–Simulink.

where [31,38]

$$I_{D1} = I_{o1}\left[\exp\left(\frac{V_{PV} + I_{PV}R_s}{a_1 V_{T1}}\right) - 1\right],$$

$$I_{D2} = I_{o2}\left[\exp\left(\frac{V_{PI_{o1}V} + I_{PV}R_s}{a_2 V_{T2}}\right) - 1\right] \quad (2)$$

and I_{Ph} is the photon current generated by the incident light, and I_{o2} are the reverse saturation currents of diode 1 and diode 2, a_1 and a_2 are the diode ideality constants , V_{T1} and V_{T2} are the thermal voltages, considering one module and given as follows [31]:

$$V_{T1} = V_{T2} = N_s \frac{KT}{q} \quad (3)$$

where N_s is number of series cells per module, q is the electron charge $(1.6021765 \times 10^{-19}$ C), K is the Boltzmann constant $(1.38065 \times 10^{-23}$ J/K) and T is the P–N junction temperature in Kelvin (K).

The value of photon current (I_{Ph}) depends on the temperature and solar radiation, and can be found using the following equation [31,39]:

$$I_{Ph} = (I_{Ph-STC} + K_I(T - T_{STC}))\frac{G}{G_{STC}} \quad (4)$$

where I_{Ph-STC} is the photon current at standard test conditions (solar radiation at standard test conditions (G_{STC}) = 1000 W/m^2, temperature at standard test conditions (T_{STC}) = 25 °C), and K_I is the current temperature coefficient in (A/°C), normally provided by the manufacturer). I_{Ph-STC} can be found using the following equation:

$$I_{Ph-STC} = I_{SC-STC}\frac{R_P + R_S}{R_P} \quad (5)$$

where I_{SC-STC} is the short circuit current at standard test conditions (given by manufacture).

The reverse saturation current of any of the diodes (I_o) can be found using the following equation [31]:

$$I_o = \frac{I_{SC-STC} + K_I(T - T_{STC})}{\exp\left(\frac{V_{OC-STC} + K_V(T - T_{STC})}{aV_T}\right) - 1} \quad (6)$$

where V_{OC-STC} is the open circuit voltage at standard test conditions (provided by the manufacturer), and K_V is the voltage temperature coefficient (V/°C). This is a modified relation that is used to calculate the reverse saturation current, while taking into account the dependency of this current on temperature variations through short circuit current and the open circuit voltage, and their respective dependence on temperature. If dependency of open circuit voltage on solar radiation variation is taken into account, Eq. (6) becomes [27]

$$I_o = \frac{I_{SC-STC} + K_I(T - T_{STC})}{\exp\left(\frac{V_{OC-STC} + K_V(T - T_{STC}) + aV_T^* \ln(G/G_{STC})}{aV_T}\right) - 1} \quad (7)$$

The PV module output voltage (V_{PV}) and output current (I_{PV}) are interdependent, so a numerical approach shall be used to calculate the I–V characteristic and the P–V characteristic of the module for the entire range of currents (from 0 to I_{SC}), and for the entire range of voltages (from 0 to V_{OC}). As surmised from Eq. (1), no direct solution exists for this equation, since I_{PV} is a function of (V_{PV} and I_{PV}), and V_{PV} is function of (V_{PV} and I_{PV}). This interdependent relation shall appear in the developed algorithm.

3.2. Genetic algorithm implementation to evaluate PV module parameters

According to Eqs. (1) and (2), which are used to represent the two-diode model, seven parameters are required to calculate either the current or voltage output from the PV module. These parameters are Iph, Io1, Io2, a1, a2, R_S, and R_p. Actually, if a1, a2, R_S, and R_p are known, then according to Eqs. (4)–(6), the values of Iph, Io1, and Io2 can be calculated. Therefore, there are two possibilities in determining the values of Iph, Io1, and Io2 using the approach developed in this paper. The first possibility is by considering them to be within the decision vector, as they form the specifications of the PV module, and the genetic algorithm specifies values for each of them alongside other parameters. The other possibility depends on the fact that their values can be calculated if the ideality factor, the series and the shunt resistances are known. In this case, values for the other parameters are specified by the genetic algorithm, and their corresponding values are accordingly calculated.

For a single-diode model, five parameters are required to be calculated. As previously mentioned, if a1, R_S, and R_p are known, then Iph and Io1 can be determined.

Different cases are tested for each model for comparison purposes, in order to find the best case that accurately and precisely models the PV panel. Taking into account previous considerations, the decision vector used in the genetic algorithm for a two-diode model DV_{2d} is given as:

$$DV_{2d} = [a1, a2, R_s, R_p] \quad (8)$$

While the decision vector for a single-diode model DV_{1d} is given as:

$$DV_{1d} = [a1, R_s, R_p] \quad (9)$$

If the reverse saturation currents and the photon current are considered within the decision vector, the modified decision vector for a two-diode model DV_{2d-m} is given as:

$$DV_{2d-m} = [I_{ph}, I_{o1}, I_{o2}, a1, a2, R_s, R_p] \quad (10)$$

and the modified decision vector for a single-diode model DV_{1d-m} is given as:

$$DV_{1d-m} = [I_{ph}, I_{o1}, a1, R_s, R_p] \quad (11)$$

The objective function is the average of absolute errors between the actual current (measured or from manufacturer datasheet) and the calculated current. This error is calculated at different values of voltage, solar radiation and temperature. So

$$Error_{ave} = \sum_{j=1}^{p} abs(I_j(curve) - I_j(V_j, G_j, T_j, DV))/p \quad (12)$$

where p is the number of points taken into account, $I_j(curve)$ is the current measured or read from the manufacturer datasheet, $I_j(V_j, G_j, T_j, DV)$ is the current calculated at the voltage V_j, the solar radiation G_j, the temperature T_j, and the corresponding decision vector DV values specified by the genetic algorithm.

To calculate the PV current $I_j(V_j, G_j, T_j, DV)$, Eq. (1) or Eq. (2) shall be used in accordance to the model used in the analysis. These equations do not have a direct solution, due to the fact that the PV current is a function of PV voltage and current, $I_{Pv} = f(I_{pv}, V_{pv})$. Instead, numerical methods should be used to solve any of these two equations, with the Newton–Raphson method being chosen preferred. The PV current I_{pv} that satisfies this equation at certain voltage V_{pv} and certain values for other variables and constants can be calculated by numerically solving the equation

$$h(I_{pv}, V_{pv}) = I_{pv} - f(I_{pv}, V_{pv}) = 0 \quad (13)$$

So, by Newton–Raphson

$$I_{pv_{n+1}} = I_{pv_n} - \left(\frac{h(I_{pv}, V_{pv})}{\frac{dh(I_{pv}, V_{pv})}{dI_{pv}}}\right)_{at I_{pv} = I_{pv_n}} \quad (14)$$

where I_{pvn} is the present value, and $I_{pv_{n+1}}$ is the next value. The PV current can be iteratively determined, and the number of iterations is determined in such a way that the absolute error between the present calculated value and the previous one is less than a certain specified tolerance.

In the following two subsections, a MATLAB code is developed to evaluate the average error fitness function. This MATLAB code is a function called that will be called by the optimization Toolbox whenever the genetic algorithm Toolbox libraries is being used, or if it is included in the genetic algorithm developed code. In this

Table 1
Specifications of the analyzed three types of PV modules.

| Parameter	PV Type					
	Mono-crystalline Sanyo – HIT 215		Poly-crystalline Kyocera – KC200GT		Thin-film shell solar – ST 40	
	Datasheet	Simulation	Datasheet	Simulation	Datasheet	Simulation
I_{sc_stc} (A)	5.61	5.61	8.21	8.209	2.68	2.68
V_{oc_stc} (V)	51.6	51.6	32.9	32.9	23.3	23.3
I_{mp} (A)	5.13	5.131	7.61	7.61	2.36	2.36
V_{mp} (V)	42	42	26.3	26.3	16.9	16.9
P_{max}	215	215.5	200	200.2	39.9	39.88
k_V (V/°C)	−0.143		−0.123		−0.1	
K_I (A/°C)	0.00196		0.0032		0.00035	
N_s	72		54		42	
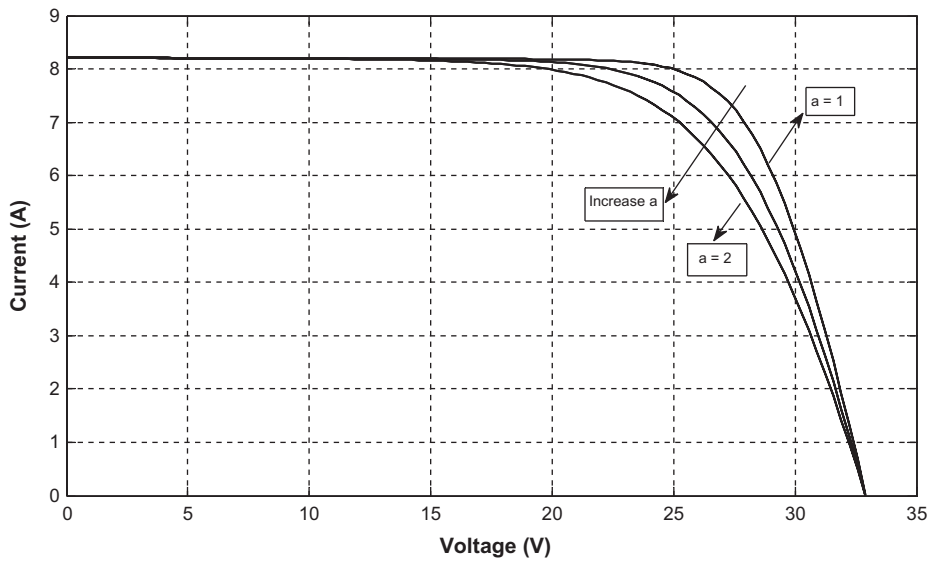
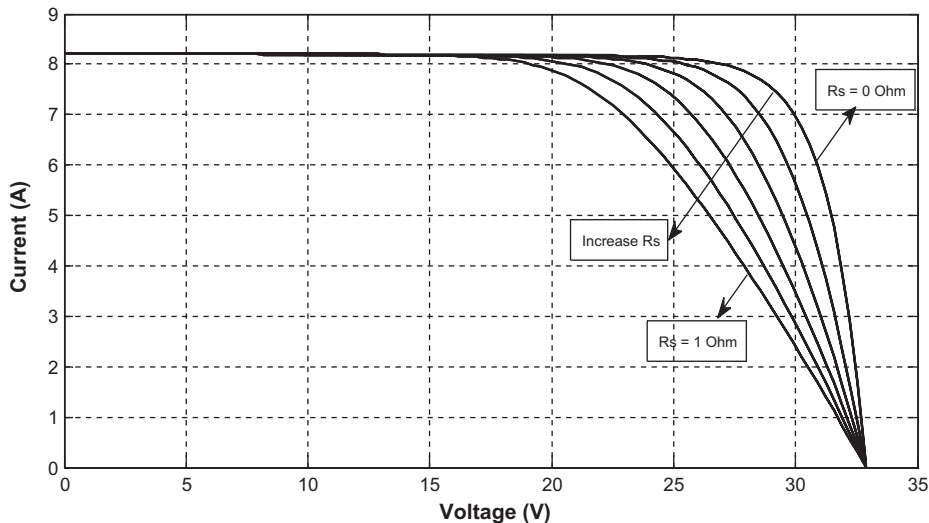**Fig. 7.** Effect of ideality factor variation on I–V curve.

Fig. 8. Effect of series resistance variation on I–V curve.

code function, different constants and parameters of the model are defined.

For different voltages, mainly at $V_{pv} = 0$, V_{mp}, and V_{OC} V, and at different solar radiation levels, mainly at $G = 1000$, 800, 600, 400, 200 W/m^2, and at different temperatures mainly at $T = 25$, 50, 75 °C, the PV current I_{pv} is calculated using Eq. (14). This current is calculated at different points, with a number of these points equaling p, and the corresponding average error objective function is calculated according to Eq. (12).

The lower and upper constraints for some of the variables constructing the decision vector are common for the different types of PV modules, while the remaining variables have lower and upper constraints, according to the PV type and manufacturer. In this study, the diode ideality constants (a_1, a_2) have lower and upper constrains between 1 and 2. The series resistance R_S usually has lower and upper constraints of between 0.01Ω and 1.2Ω, while the shunt resistance R_p usually has lower and upper constraints

of between 50 Ω and 1000 Ω, but these values can be altered according to the results of the genetic algorithm.

Some PV manufacturers do not provide the datasheet illustrating the I–V and P–V curves at different radiation levels or different temperature values. They only provide K_V, K_I, V_{OC-STC}, I_{SC-STC} and V_{mp}, I_{mp} at standard test conditions. In this case, Eq. (15)–(18) can be used to calculate the open circuit voltage and the short circuit current at different radiation levels and different temperatures [19]

$$I_{SC}(G,T) = I_{SC-STC} * (G/G_{STC}) + K_I * (T - T_{STC}) \tag{15}$$

$$V_{OC}(G,T) = V_{OC-STC} - K_V * (T - T_{STC}) + a * V_T * \ln(G/G_{STC}) \tag{16}$$

$$I_{mp}(G,T) = I_{mp-STC} * (G/G_{STC}) \tag{17}$$

$$V_{mp}(G,T) = V_{mp-STC} - K_V * (T - T_{STC}) \tag{18}$$

These equations can be used even when the data sheets are available, instead of using datasheet curves to read currents at different voltages, radiation levels and temperature values. Actually, using these equations provide values of decision vector parameters that accurately model the PV module, as illustrated in the following section.

4. Results and discussion

In order to validate the adopted model, the results of the simulation of the model using Matlab–Simulink are compared with the manufacturer's datasheet. Three types of PV modules, using different technologies, are used for this purpose, which include the mono-crystalline (from Sanyo (HIT – 215)), multi-crystalline (from Kyocera (KC200GT)), and thin-film (from Shell Solar (ST 40)) types. Table 1 shows the constants and parameters for these types, with the Data sheets downloaded from the companies' web sites. On top of the datasheet values, this table also includes the simulation results for these three types of PV modules at standard test conditions. It is fairly obvious from comparing these values that the results of the simulation agree with the data sheet values.
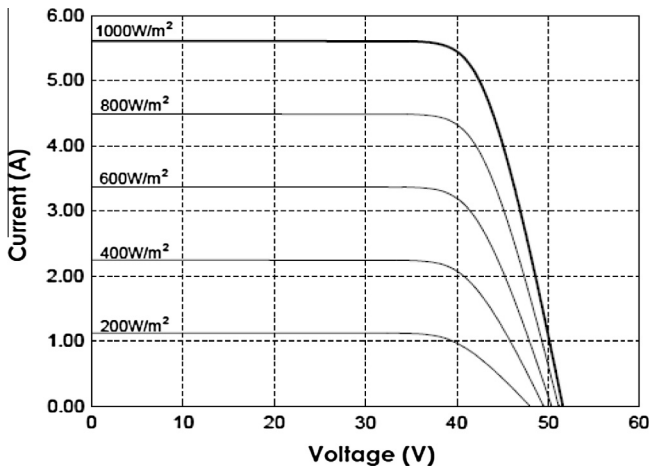

Fig. 9. I–V curves for Sanyo – HIT 215 module from manufacturer at different solar radiation levels and $T = 25$ °C.

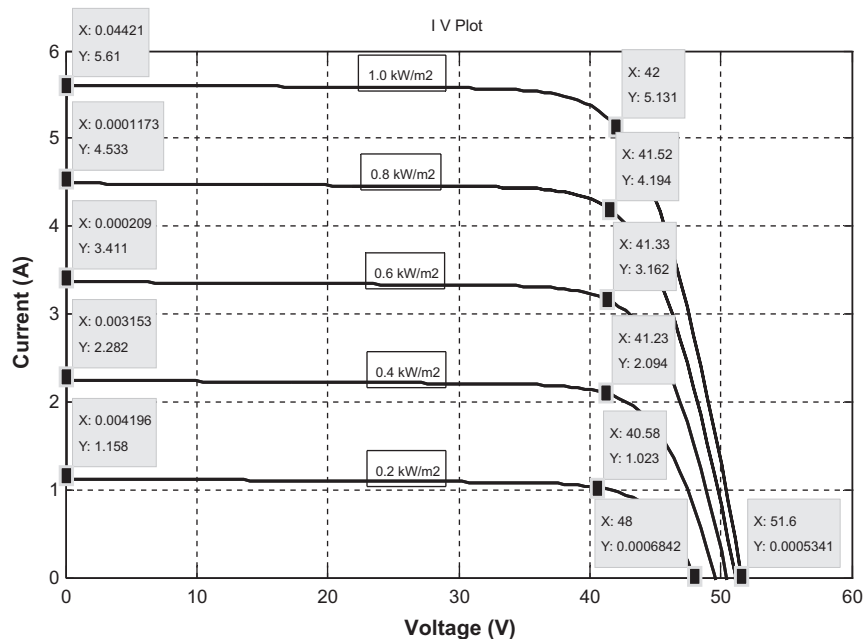**Fig. 10.** Simulation I–V curves for Sanyo – HIT 215 module at different solar radiation levels and $T = 25$ °C.

Table 2
Comparison between data sheet and simulation results for Sanyo – HIT 215 module at different radiation levels.

Quantity	G = 1 kW			G = 0.6 kW			G = 0.2 kW		
	Data sheet	Simulation	Abs. error	Data sheet	Simulation	Abs. error	Data sheet	Simulation	Abs. error
V_{oc} (V)	51.6	51.6	0	50.43	50.47	0.04	47.94	48	0.06
I_{sc} (A)	5.61	5.61	0	3.4	3.411	0.011	1.145	1.158	0.015
I_{mp} (A)	5.13	5.131	0.001	1.98	2.094	0.114	0.905	1.023	0.118

4.1. Effect of variation of parameters (a, R_S, R_p)

The effect of varying different variables constructing the decision vector on the characteristic curves of the PV module differs, and the effect of varying the ideality factor on the I–V is shown in Fig. 7. It is obvious from the figure that increasing the ideality
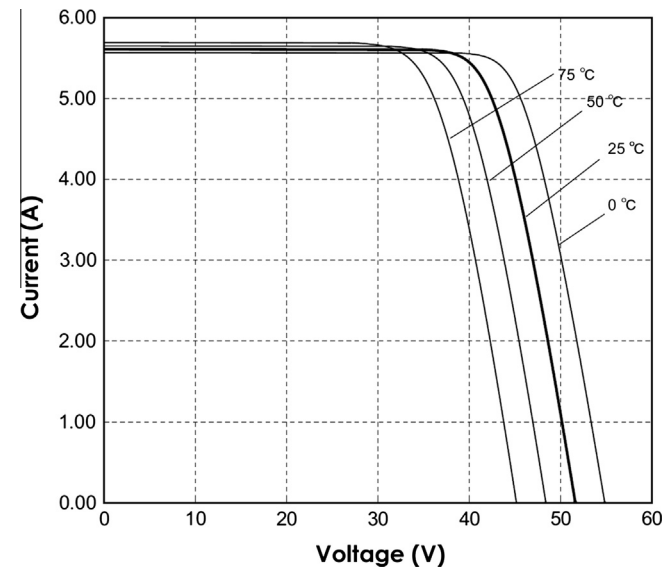

Fig. 11. I–V curves for Sanyo – HIT 215 from manufacturer at different temperatures and at $G = 1$ kW/m².

factor decreases the values of voltage, current and consequently, power, at the maximum point. Fig. 8 shows the effect of varying the series resistance on the I–V curve. This figure illustrates that as the R_S increases, the values of voltage, current and power at the maximum point also decrease. In addition, it is also observed that varying the values of both ideality factor and series resistance caused a noticeable effect at the region of the maximum power point. Finally, the effect of varying R_p on the I–V curve of a PV module was also studied, but this effect was barely noticeable. These comparisons were done on a Kyocera (KC200GT) panel, at standard test conditions. This panel was also selected for the validation of the results of the developed approach.

4.2. Results of genetic algorithm

Different cases were taken into account while using the genetic algorithm to extract the optimal parameters of the PV module. The purpose of analyzing different cases is to specify the most optimal case that enables the extraction of the most precise parameters of PV module model, which when used in the simulation program, provides the results that agrees with the datasheet information.

Case 1: The usage of a single-diode model and the optimization is done using Toolbox optimization Matlab library:

In this case, a single-diode model and a Toolbox optimization Matlab library were used. The results obtained from this case are deemed the most accurate. The Diode ideality factor (a), series resistance (R_S) and shunt resistance (Rsh) are the calculated parameters using the genetic algorithm.

For a Mono-Crystalline PV (Sanyo – HIT 215), the values of the parameters are [a = 1.178, R_S = 0.782 Ω, Rsh = 852.177 Ω, with an
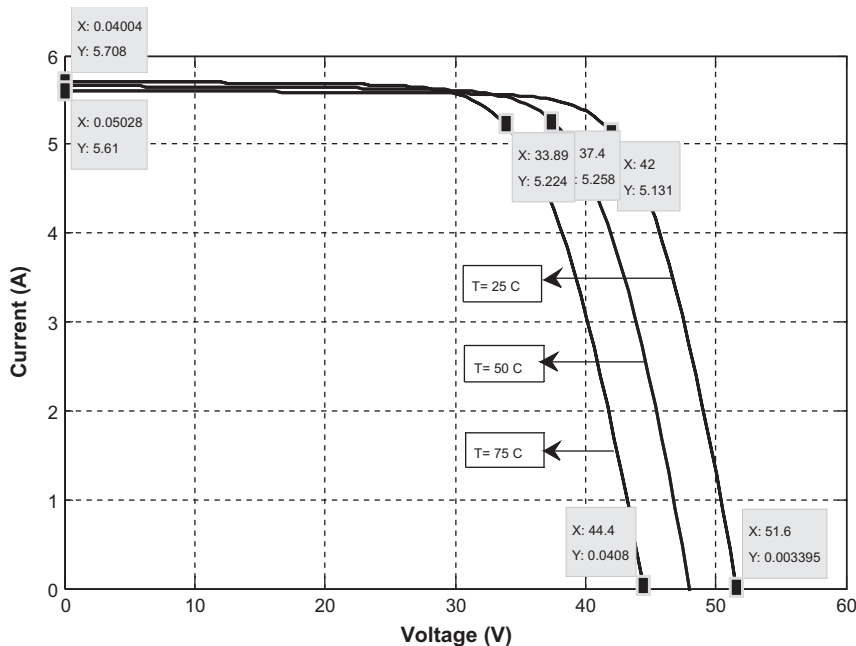

Fig. 12. Simulation I–V curves for Sanyo – HIT 215 at different temperatures and at $G = 1$ kW/m².

average absolute error = 0.016615]. Fig. 9 shows the I–V curves taken from the manufacturer data sheet for the different radiation levels, while Fig. 10 shows the simulation results that take into account the values of the parameters being given before. The values of the voltages at maximum power points are read from the simulation P–V curve, which were not provided by the manufacturer. From the two figures, one can observe the similarity of the results at different radiation levels. Table 2 summarizes a comparison between the results of the two graphs at open circuit, short circuit and maximum points. The largest absolute error in the current occurs at the region of the maximum power point, and as it is obvious from the graphs and the table, it increases as the radiation decreases, but still possesses small values. Fig. 11 shows the I–V curve for the same PV module at different temperatures, while Fig. 12 shows the simulation results for the same module. Detailed graphs of error as function of voltage for different radiation levels and different temperature values are illustrated later in this section.

For a Multi-Crystalline PV (Kyocera – Kyocera – KC200GT), the values of the parameters are [$a = 1.106$, $R_S = 0.331\,\Omega$, $Rsh = 883.925\,\Omega$, with an average absolute error = 0.0152]. Fig. 13 shows the I–V curve obtained from the manufacturer data sheet for different temperature levels, while Fig. 14 shows the simulation

results that take into account the values of parameters that were previously provided. The values of the voltages at maximum power points are read from the simulation P–V curve, which are not provided by the manufacturer. Table 3 summarizes a comparison between the results of the two graphs at open circuit, short circuit and maximum points. From the two figures, one can observe the similarity of the results at different temperature levels. The largest absolute error in the current occurs at the region of maximum power point, and as it is obvious from the graphs and the table, it increases as radiation decreases, but still possesses small values. Fig. 15 shows the I–V curves for the same PV module at different radiation levels, while Fig. 16 shows the simulation results for the same module. Table 4 summarizes a comparison between the results of the two graphs at open circuit, short circuit and maximum points.

For a thin film PV (Shell Solar – ST 40), the values of the parameters are [$a = 1.558$, $R_S = 1.149\,\Omega$, $Rsh = 860.75\,\Omega$, with an average absolute error = 0.0094]. Fig. 17 shows the I–V curve taken from the manufacturer's data sheet for different temperature levels, while Fig. 18 shows the simulation results, taking into account the values of the parameters given before. The values of voltages at maximum power points are read from the simulation P–V curve. Table 5 summarizes a comparison between the results of the two graphs at open circuit, short circuit and maximum points. From the two figures, one can observe the similarity of the results at different temperature levels. Furthermore, the manufacturer provides the value for the series resistance, which equals to 1.14 Ω. This value is consistent with the value that was computed using the developed approach.

Case 2: Is similar to case 1, but the optimization is done via the developed Matlab code.

For this case, a Kyocera module is also taken into account for comparison purposes. The values of the parameters that are extracted by the genetic algorithm code are [$a = 1.107$, $R_S = 0.3395$, $Rsh = 870.27$ with an average absolute error = 0.0153]. For this case, Fig. 19 shows the I–V curves for different radiation levels. The results of this figure can be compared with the results of the Toolbox optimization, shown in Fig. 16. The comparison shows that the corresponding values in the two figures are almost similar. Fig. 20 shows the value of the average absolute error as a function of the number of generations. This graph is obtained via the devel-
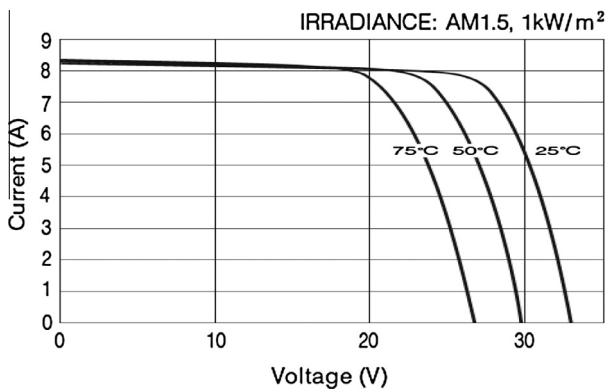

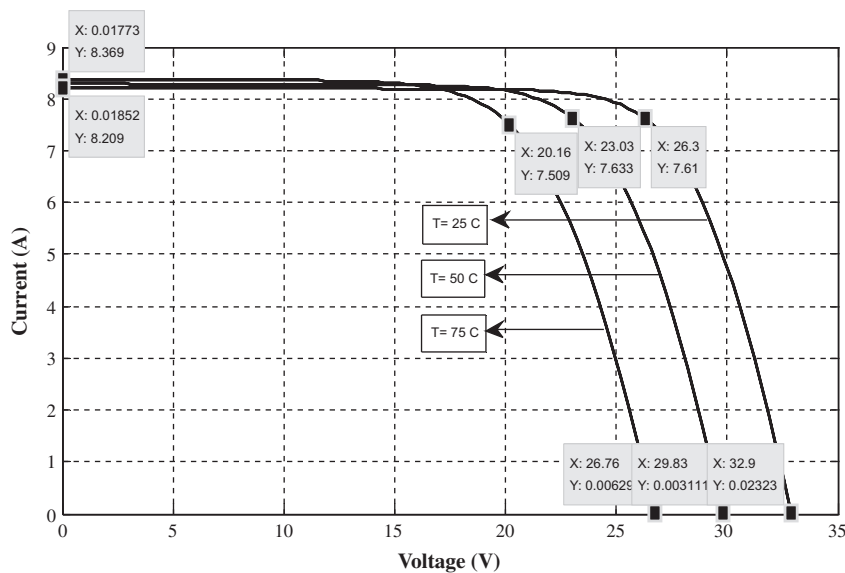**Fig. 13.** I–V curves for Kyocera – KC200GT from manufacturer at different temperatures and at $G = 1$ kW/m^2.

Fig. 14. Simulation I–V curves for Kyocera – KC200GT at different temperatures and at $G = 1$ kW/m^2.

Table 3
Comparison between data sheet and simulation results for Kyocera – KC200GT module at different temperature values.

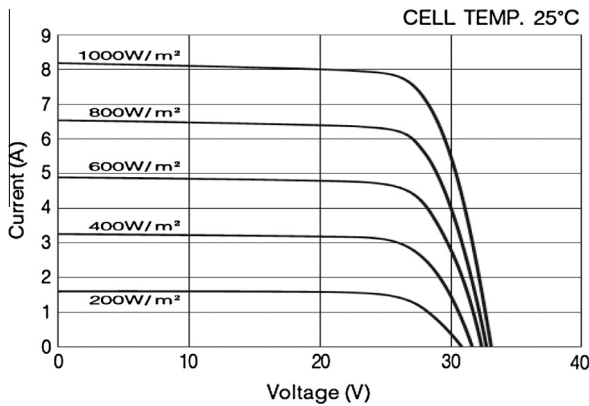| Quantity	$T = 25\,°C$			$T = 50\,°C$			$T = 75\,°C$		
	Data sheet	Simulation	Abs. error	Data sheet	Simulation	Abs. error	Data sheet	Simulation	Abs. error
V_{oc} (V)	32.9	32.9	0	29.78	29.83	0.05	26.7	26.76	0.06
I_{sc} (A)	8.2	8.209	0.009	8.298	8.312	0.014	8.397	8.369	0.028
I_{mp} (A)	7.61	7.61	0	7.72	7.633	0.078	7.68	7.509	0.171

Fig. 15. I–V curves for Kyocera – KC200GT 215 module from manufacturer at different solar radiation levels and $T = 25\,°C$.

oped Matlab code. It is obvious that after about fifteen generations, the optimized function obtains its final value.

Case 3: In this case, a two-diode model is used, and the decision vector is made up of six parameters. The optimization Toolbox is used, and the Kyocera module is also used for comparison purposes. The values of the parameters extracted by the genetic algorithm code are [$a1 = 1.112$, $a2 = 1.377$, $R_S = 0.29\,\Omega$, $Rsh = 480.496\,\Omega$, $Io1 = 4.23 \times 10^{-9}$ A, $Io2 = 9.1478 \times 10^{-9}$ A, with an average absolute error = 0.02]. For this case, Fig. 21 shows the I–V curves for different radiation levels. The results can be compared to the results of the Toolbox optimization that are shown in Fig. 16 for the case of a single-diode model. The comparison shows that the corresponding values in the two figures are almost similar, while the single-diode model provides a more accurate result compared to the datasheet values, with an average absolute error also being smaller.

The I–V curves shown in case-1's results accurately match the data sheet information for all radiation levels and temperature values, along with all types of modules. The absolute error in the PV current does not exceed 0.20 A, even in its worst case scenario (for Kyocera at temperature = 75\,°C), while in other cases, it is invariably less. A detailed graph, illustrating the absolute error as a function of voltage for different radiation levels, and at temperatures equaling 25\,°C, is shown in Fig. 22, while Fig. 23 illustrates it for different temperature levels at solar radiations equaling 1 kW/m². These two graphs illustrate the agreement in values between the datasheet information and the simulation results. It is also
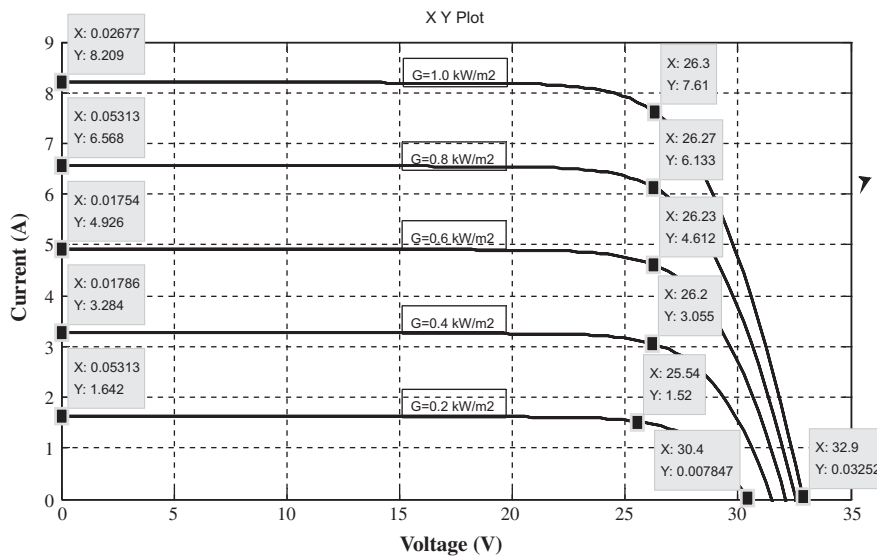

Fig. 16. Simulation I–V curves for Kyocera – KC200GT 215 module at different solar radiation levels and $T = 25\,°C$ – (3 parameters).

Table 4
Comparison between data sheet and simulation results for Kyocera – KC200GT module at different radiation levels.

Quantity	$G = 1\,kW$			$G = 0.6\,kW$			$G = 0.2\,kW$		
	Data sheet	Simulation	Abs. error	Data sheet	Simulation	Abs. error	Data sheet	Simulation	Abs. error
V_{oc} (V)	32.9	32.9	0	32.07	32.12	0.05	30.46	30.4	0.06
I_{sc} (A)	8.2	8.209	0.009	4.9	4.926	0.026	1.595	1.642	0.047
I_{mp} (A)	7.61	7.61	0	4.62	4.612	0.008	1.53	1.52	0.010

Fig. 17. I–V curves for shell solar – ST 40 from manufacturer at different temperatures and at $G = 1$ kW/m^2.

results of the study presented in Ref. [27] for different types of PV modules, although in the developed approach presented in this manuscript, certain constant value was calculated for each parameter for the whole range of solar radiation and temperatures. For a thin-film PV (ST40), authors of Ref. [27] found values for the series resistance to be within the range of (0.71–0.99 Ω), and presented a value for this resistance, which equals to 0.092 Ω using the R_S-model. In the developed approach in this manuscript, this value equals to 1.149 Ω, and it is consistent with the value provided by the manufacturer. The results are also consistent with results of Ref. [30], where the effect of the temperature on the ideality factor and series resistance was taken into consideration. Authors of Ref. [31] presented their results in a graphical form. The presented curves in this reference included the results of the absolute error in the current for the approach developed in this reference, and the results of another approach. The results were for the Kyocera PV module (KC200GT) at standard test conditions. The maximum recorded absolute error in this reference was about 0.45 A, while it was about 0.88 A for the other presented approach. In the developed approach presented in this manuscript, it was about 0.02 A. The same comparison was conducted with the results of Ref. [22], where the maximum recorded absolute error for the current was about 0.2 A for the Kyocera PV module (KC200GT) at standard test conditions, and it was greater than this value for the other two methods presented in the same reference.

Many attempts were made to find the execution time to obtain the model parameters. It was found that this time, in most cases, it is less than 4 s. However, as this developed approach uses the specifications of any solar module given by the manufacturer to extract global values of the parameters that suit the entire range of solar radiation and temperature variations, these parameters can be firstly calculated (off-line). This means that in this approach, there is no need for real time modeling. In other approaches where the parameter values change with solar radiation and temperatures variations, real-time modeling is required. In these cases, the mod-
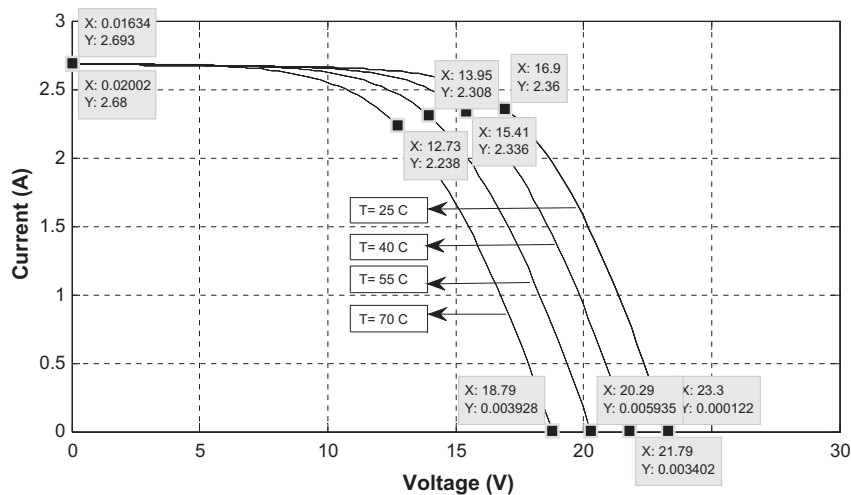
fairly obvious that the maximum error occurs at the region of the maximum power point, where the curvature of the curve is largely affected by the values of the PV parameters.

Certain value for each parameter was extracted using this approach, which shows strong agreement of the results with the data sheet information. In this approach, solar radiation and temperature variations were incorporated into the calculation while formulating the average absolute error fitness function in order to compute the optimized values for different parameters. A value that deals with the entire range for solar radiation and temperatures was therefore calculated for each parameter. In Ref. [27], the used approach enabled the computation of the values of the parameters that change with solar radiation variation and/or temperature variation. The results of this study are consistent with the

Fig. 18. Simulation I–V curves for shell solar – ST 40 at different temperatures and at $G = 1$ kW/m^2.

Table 5
Comparison between data sheet and simulation results for Shell Solar – ST 40 module at different temperature values.

Quantity	$T = 25$ °C			$T = 40$ °C			$T = 55$ °C		
	Data sheet	Simulation	Abs. error	Data sheet	Simulation	Abs. error	Data sheet	Simulation	Abs. error
V_{oc} (V)	23.3	23.3	0	22.03	21.79	0.24	20.75	20.29	0.46
I_{sc} (A)	2.68	2.68	0	2.683	2.685	0.002	2.687	2.690	0.003
I_{mp} (A)	2.36	2.36	0	2.35	2.336	0.006	2.323	2.308	0.015

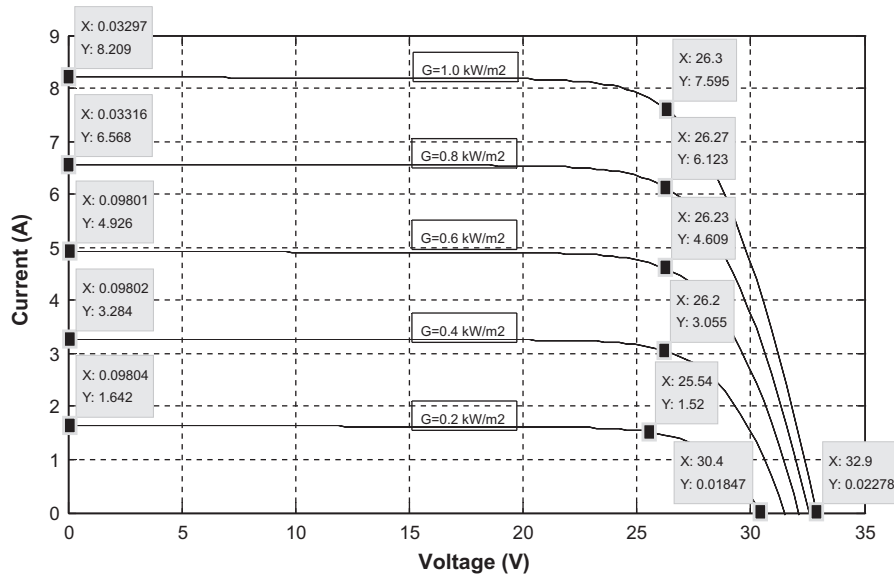**Fig. 19.** Simulation I–V curves for Kyocera – KC200GT 215 module at different solar radiation levels and *T* = 25 °C – using developed code for genetic algorithm.
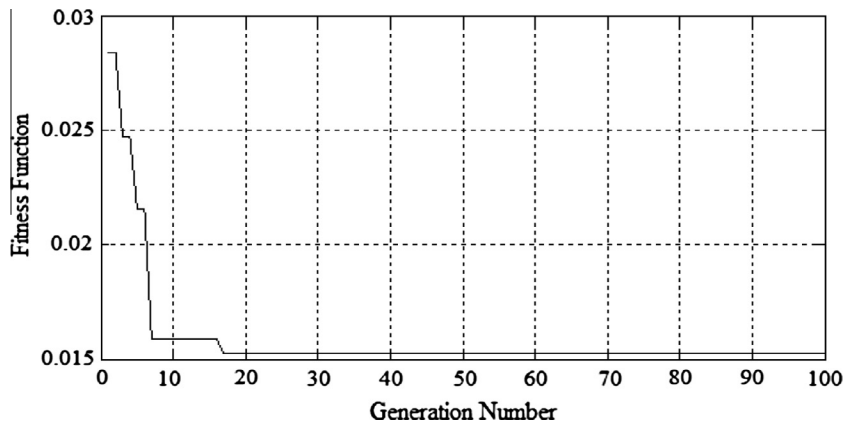

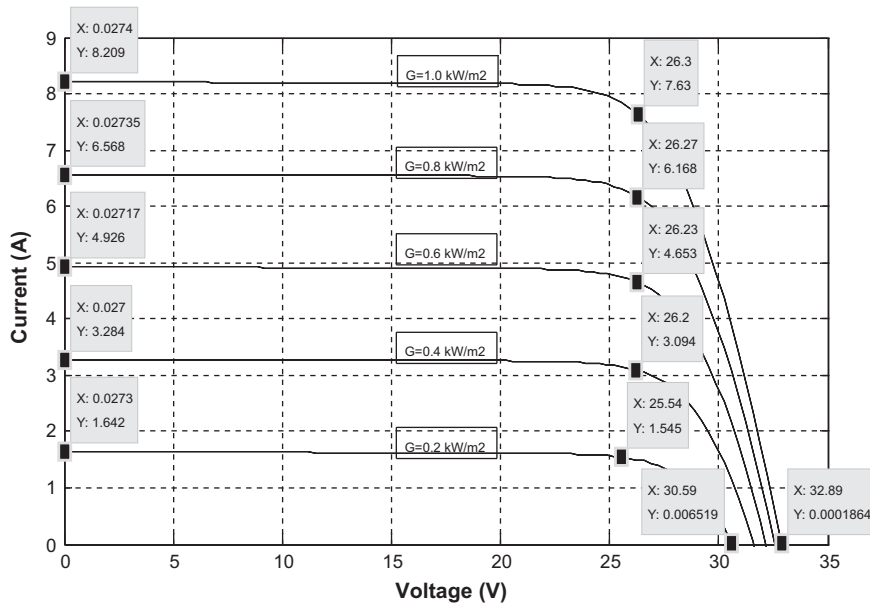**Fig. 20.** Average absolute error as a function of generation number.

Fig. 21. Simulation I–V curves for Kyocera – KC200GT 215 module at different solar radiation levels and *T* = 25 °C – (6 parameters).

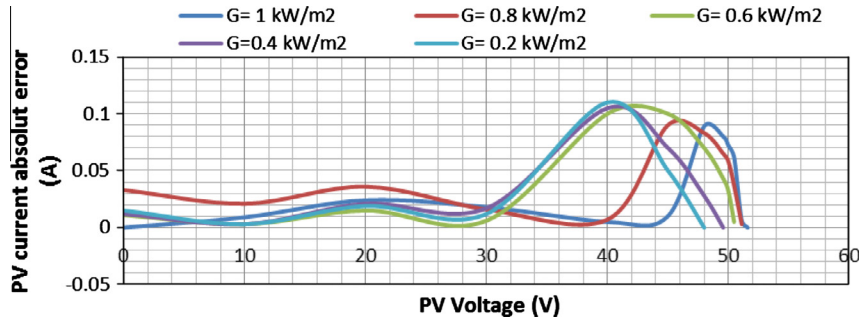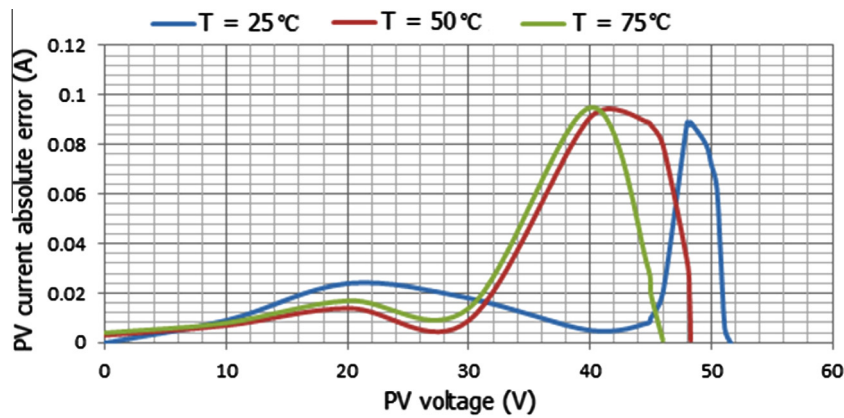**Fig. 22.** Absolute error in PV current for different radiation levels at T = 25 °C for Sanyo – HIT 215 module.

Fig. 23. Absolute error in PV current for different temperature values at G = 1 kW/m^2 for Sanyo – HIT 215 module.

eling approach shall be fast enough to deal with real time operation.

4.3. Validation of the results of the developed model for partial shading

In partial shading, different parts of the PV array are exposed upon different radiation levels. If the approach is able to provide an accurate model of the PV panel at different solar radiation and temperature values, this developed model can be satisfactorily applied in the case of partial shading.

As it was earlier mentioned in this work, the developed approach provides the parameters for the PV model that suit the entire range of the solar radiation and temperature fluctuations. So, the developed model described in this work can be accurately used for this purpose. Actually, there is no need for real time modeling to be utilized while using the model developed by this approach, since this model is appropriate for different radiation and temperature levels. This is so due to the fact that there is no need to adapt the values of model's parameters to real time operation.

In order to validate the ability of this developed model to deal with partial shading, a PV array configuration composed of 20 PV panels and connected in series to form a string and three strings, are connected in parallel. This case was studied in detail by Ref. [22], where the SM55-Siemens PV panel was selected to validate the partial shading modeling. The authors presented the results of the developed model in this reference where a two-diode model is used alongside results of other previous studies. Four shading patterns affecting this array were assumed. Specific radiation levels for each shading pattern were selected, and different temperature values were also considered. Fig. 24 shows the series parallel connections of the 20 ∗ 3 PV array, while Table 6 displays the simulation results of this work for selected cases of partial shading

patterns at different temperatures alongside the results presented in the same mentioned reference. The simulations showed satisfactory results compared to the results presented in this reference. Fig. 25 shows the P–V curve of partial shading case 1, mentioned in Table 6.

The values of the parameters that were extracted by the genetic algorithm for this panel are [a = 1.107, R_S = 0.551, Rsh = 940.52 with an average absolute error = 0.008]. The simulation results in this manuscript that uses these parameters showed that this array is capable of generating 3292 W, at a voltage of 347.2 V, at maximum power point at standard test conditions. As provided by the manufacturer's datasheet, the maximum power point voltage and current at standard test conditions for this panel are 17.4 V and 3.15 A, respectively. According to these specifications, this array can produce a power of 3288 W at 348 V, which are very close to the simulation results, while the simulation results presented by Ref. [22] for power and voltage are 3220 W and 350 V, respectively.
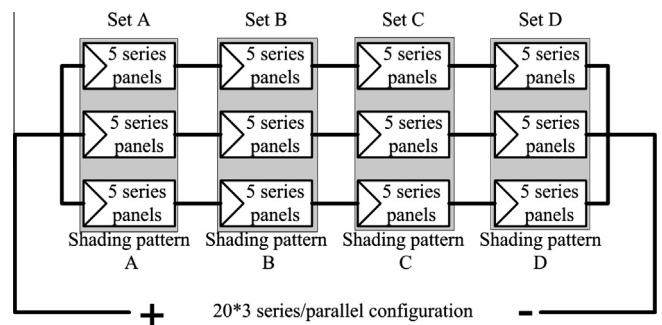

Fig. 24. The series parallel connections for the 20 ∗ 3 array.

Table 6
The voltage V_{mp} and the power P_{mp} outputs of a 20 * 3 PV array at global maximum power point under different shading patterns at different temperatures.

| Case	T (°C)	Shading pattern 1 means 1000 W/m²				Two diode model [22]		Results of studies presented in Ref. [22]				Proposed approach	
								Artificial neural network		R_S-model			
		A	B	C	D	V_{mp} (V)	P_{mp} (W)	V_{mp} (V)	P_{mp} (W)	V_{mp} (V)	P_{mp} (W)	V_{mp} (V)	P_{mp} (W)
1	25	1	0.75	0.5	0.25	275	1359.6	276.38	1383.1	271	1350.8	271.8	1376.8
2	25	0.75	0.5	0.2	0.1	177	867.6	172.46	847.77	172	844.17	179.7	895.79
3	50	0.8	0.6	0.4	0.2	243	965.92	241.01	964.26	236	940.89	254.99	1028.04
4	75	0.9	0.6	0.3	0.1	158	935.20	150.35	885.98	156	914.9	147.86	885.11
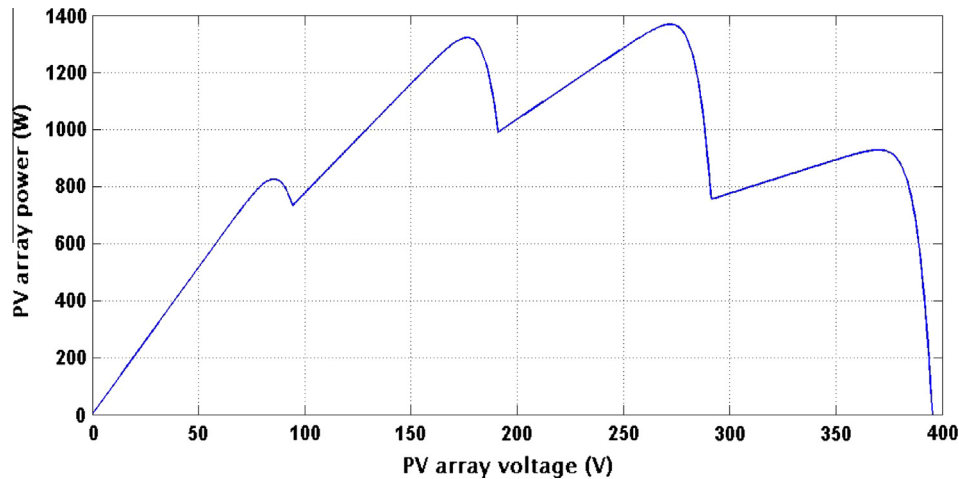
Fig. 25. The P–V curve of case 1 mentioned in Table 6.

The values for power and voltage under different shading patterns presented in Ref. [22] are the simulation results of approaches, developed by the authors of this reference and the authors of other studies, cited by the same reference.

The developed model in this manuscript showed accurate results for the proposed (20 * 3) array under standard test conditions, as previously discussed. Furthermore, the SM55 PV panel manufacturer provides a datasheet, including I–V curves of one module at two radiation levels (1000 W and 800 W), and three temperature values (25, 45 and 60 °C). The simulation results at ($G = 1000$ W/m², $T = 60$ °C) and at ($G = 800$ W/m², $T = 45$ °C) are consistent with the datasheet's information.

5. Conclusions

In this paper, a modeling method based on the genetic algorithm is proposed. The values of the PV module parameters were computed in such a way that the error between the simulation results and the data sheet information is minimized. A global optimization for the values of the parameters was realized, so the values extracted using this algorithm are applicable for the entire range of the solar radiation and temperatures. The information provided by the manufacturer's data sheet of a certain PV module is the only requirement for this approach. The Matlab–Simulink environment was used to simulate the operation of the PV module using the parameters obtained by the genetic algorithm. The accuracy evaluation of this approach was achieved by comparing the results of the simulation based on the extracted parameters with the manufacturer's data sheet information. The result validation was conducted for three types of PV modules from different technologies (mono-crystalline, poly-crystalline and thin-film). Different cases were also analyzed for the purpose of comparison. It was found that the error between the simulation results, based on the ex-

tracted parameters and the data sheet was minuscule for different simulated types at different temperatures and different solar radiation. The most accurate results (achieving least error) were obtained using single-diode model with three extracted parameters (ideality factor, series resistance and shunt resistance). The photon current and the saturation current of the model were calculated depending on the optimally extracted parameters. The effectiveness of the model developed by this approach to predict the performance of the PV system under partial shading conditions was also approved. The accurate modeling of any PV module is an important tool required for any further studies concerning PV applications, so this approach can be used as valuable tool for this exact purpose.

Acknowledgements

References

[1] Kaldellis JK, Zafirakis D, Kaldelli EL, Kavadias K. Cost benefit analysis of a photovoltaic-energy storage electrification solution for remote islands. Renew Energy 2009;34:1299–311.
[2] Bhandari R, Stadler I. Electrification using solar photovoltaic systems in Nepal. Appl. Energy 2011;88:458–65.
[3] Liu G, Nguang SK, Partridge A. A general modeling method for I–V characteristics of geometrically and electrically configured photovoltaic arrays. Energy Convers Manage 2011;52:3439–45.
[4] Hamad AA, Alsaad MA. A software application for energy flow simulation of a grid connected photovoltaic system. Energy Convers Manage 2010;51:1684–9.
[5] Chong WT, Naghavi MS, Poh SC, Mahlia TMI, Pan KC. Techno-economic analysis of a wind–solar hybrid renewable energy system with rainwater collection feature for urban high-rise application. Appl Energy 2011;88:4067–77.

[6] Ismail MS, Moghavvemi M, Mahlia TMI. Design of a PV/diesel standalone hybrid system for a remote community in Palestine. J Asian Sci Res 2012;2:599–606.

[7] Dagdougui H, Minciardi R, Ouammi A, Robba M, Sacile R. Modeling and optimization of a hybrid system for the energy supply of a "Green" building. Energy Convers Manage 2012;64:351–63.

[8] Ayompe LM, Duffy A, McCormack SJ, Conlon M. Measured performance of a 1.72 kW rooftop grid connected photovoltaic system in Ireland. Energy Convers Manage 2011;52:816–25.

[9] Daud A, Ismail MS. Design of isolated hybrid systems minimizing costs and pollutant emissions. Renew Energy 2012;44:215–24.

[10] Jacobus H, Lin B, Jimmy DH, Ansumana R, Malanoski AP, Stenger D. Evaluating the impact of adding energy storage on the performance of a hybrid power system. Energy Convers Manage 2011;52:2604–10.

[11] Twaha S, Idris MH, Anwari M, Khairuddin A. Applying grid-connected photovoltaic system as alternative source of electricity to supplement hydro power instead of using diesel in Uganda. Energy 2012;37:185–94.

[12] Braun P, Rüther R. The role of grid-connected, building-integrated photovoltaic generation in commercial building energy and power loads in a warm and sunny climate. Energy Convers Manage 2010;51:2457–66.

[13] Bandara K, Sweet T, Ekanayake J. Photovoltaic applications for off-grid electrification using novel multi-level inverter technology with energy storage. Renew Energy 2012;37:82–8.

[14] Mellit A, Pavan AM. Performance prediction of 20 kWp grid-connected photovoltaic plant at Trieste (Italy) using artificial neural network. Energy Convers Manage 2010;51:2431–41.

[15] Al-Salaymeh A, Al-Hamamre Z, Sharaf F, Abdelkader MR. Technical and economical assessment of the utilization of photovoltaic systems in residential buildings: the case of Jordan. Energy Convers Manage 2010;51:1719–26.

[16] Avril S, Arnaud G, Florentin A, Vinard M. Multi-objective optimization of batteries and hydrogen storage technologies for remote photovoltaic systems. Energy 2010;35:5300–8.

[17] Safari S, Ardehali MM, Sirizi MJ. Particle swarm optimization based fuzzy logic controller for autonomous green power energy system with hydrogen storage. Energy Convers Manage 2013;65:41–9.

[18] Abdullah MO, Yung VC, Anyi M, Othman AK, Hamid KBA, Tarawe J. Review and comparison study of hybrid diesel/solar/hydro/fuel cell energy schemes for a rural ICT Telecenter. Energy 2010;35:639–46.

[19] Chouder A, Silvestre S, Sadaoui N, Rahmani L. Modeling and simulation of a grid connected PV system based on the evaluation of main PV module parameters. Simul Model Pract Theory 2012;20:46–58.

[20] Su Y, Chan L-C, Shu L, Tsui K-L. Real-time prediction models for output power and efficiency of grid-connected solar photovoltaic systems. Appl Energy 2012;93:319–26.

[21] Nosrat A, Pearce JM. Dispatch strategy and model for hybrid photovoltaic and trigeneration power systems. Appl Energy 2011;88:3270–6.

[22] Ishaque K, Salam Z, Taheri H. Modeling and simulation of photovoltaic (PV) system during partial shading based on a two-diode model. Simul Model Pract Theory 2011;19:1613–26.

[23] Congedo PM, Malvoni M, Mele M, Giorgi MGD. Performance measurements of monocrystalline silicon PV modules in South-eastern Italy. Energy Convers Manage 2013;68:1–10.

[24] Díez-Mediavilla M, Alonso-Tristán C, Rodríguez-Amigo MC, García-Calderón T, Dieste-Velasco MI. Performance analysis of PV plants: optimization for improving profitability. Energy Convers Manage 2012;54:17–23.

[25] Eke R, Demircan H. Performance analysis of a multi crystalline Si photovoltaic module under Mugla climatic conditions in Turkey. Energy Convers Manage 2013;65:580–6.

[26] Sera D, Teodorescu R, Rodriguez P. PV panel model based on datasheet values. In: Industrial electronics, 2007 ISIE 2007 IEEE international, symposium on 2007. p. 2392–6.

[27] Ishaque K, Salam Z. An improved modeling method to determine the model parameters of photovoltaic (PV) modules using differential evolution (DE). Solar Energy 2011;85:2349–59.

[28] Shahat AE. Maximum power point genetic identification function for photovoltaic system. IJRRAS 2010;3:264–73.

[29] Zagrouba M, Sellami A, Bouaïcha M, Ksouri M. Identification of PV solar cells and modules parameters using the genetic algorithms: application to maximum power extraction. Solar Energy 2010;84:860–6.

[30] Weidong X, Dunford WG, Capel A. A novel modeling method for photovoltaic cells. In: Power electronics specialists conference, 2004 PESC 04 2004 IEEE 35th annual, vol. 3; 2004. p. 1950–6.

[31] Villalva MG, Gazoli JR, Filho ER. Comprehensive approach to modeling and simulation of photovoltaic arrays. IEEE Trans Power Electron 2009;24:1198–208.

[32] Jervase JA, Bourdoucen H, Al-Lawati A. Solar cell parameter extraction using genetic algorithms. Meas Sci Technol 2001;12:1922–5.

[33] Almonacid F, Rus C, Hontoria L, Fuentes M, Nofuentes G. Characterisation of Si-crystalline PV modules by artificial neural networks. Renew Energy 2009;34:941–9.

[34] Shaiek Y, Smida MB, Sakly A, Mimouni MF. Comparison between conventional methods and GA approach for maximum power point tracking of shaded solar PV generators. Sol Energy 2013;90:107–22.

[35] Kadri R, Andrei H, Gaubert J-P, Ivanovici T, Champenois G, Andrei P. Modeling of the photovoltaic cell circuit parameters for optimum connection model and real-time emulator with partial shadow conditions. Energy 2012;42:57–67.

[36] Mohamed FA, Koivo HN. Online management genetic algorithms of microgrid for residential application. Energy Convers Manage 2012;64:562–8.

[37] Silva M, Morais H, Vale Z. An integrated approach for distributed energy resource short-term scheduling in smart grids considering realistic power system simulation. Energy Convers Manage 2012;64:273–88.

[38] Sandrolini L, Artioli M, Reggiani U. Numerical method for the extraction of photovoltaic module double-diode model parameters through cluster analysis. Appl Energy 2010;87:442–51.

[39] Chang TP. Output energy of a photovoltaic module mounted on a single-axis tracking system. Appl Energy 2009;86:2071–8.